International Journal of Thin Films Science and Technology

http://dx.doi.org/10.18576/ijtfst/140201

Investigation of Intensity Distribution in Image plane for Different Focus Errors in Optical System Illuminated by Coherent light Operating with an Annular Aperture

Safaa Mustafa Hameed

Department of Optics Techniques, College of Health & Medical Technology, Sawa University, Almuthana, Iraq

Received: 8 Dec. 2024, Revised: 20 Jan. 2025, Accepted: 24 Jan. 2025
Published online: 1 May 2025

Abstract: In this paper, one common kind of aberration in optical systems that can seriously impair the quality of the images taken is focus errors. This study aims to assess the impact of focus errors on the distribution of intensity in the image plane of the optical system, which is composed of a circular area nature. The Zernike coefficient W20 is used to compute quantitatively defined focus errors, and the results are verified experimentally and through simulations that use the Fresnel diffraction integral. In excellent agreement with the theoretical prediction, the measurement results confirm that the fault-free optical system generates a central peak of higher intensity (Airy disk) surrounded by a Pearly ring structure of lower intensity (Airy rings). The phenomenon of Airy rings becomes more noticeable as the central peak tends to smear more and lose intensity from W20 = 0.25 to W20 = 1.25. The image quality consequently deteriorates over time. With an NRMS error of less than 0.1 for every position error condition, the experimental results exhibit a trend that is comparable to the modulated (simulated) intensity distributions. Low-quality imaging is caused by focus errors, which play a critical role in the design, optimization, and characterization of optical systems, as supported by the aforementioned results. This offers a variety of approaches to enhance computational imaging methods and create the best possible optical designs.

Keywords: focus errors, intensity distribution, coherent illumination, circular aperture, Zernike coefficients, Airy disk, rings, resolving power, Fresnel diffraction integral, optical system design, computational imaging.

1. Intensity Distribution in the Image Plane

Numerous applications, from imaging and microscopy to optical metrology and laser material processing, depend on an understanding of the intensity distribution in optical systems. An optical system's performance level in terms of resolution, clarity, and the quality of the image it produces is determined by intensity distributions in the image plane [1]. When an optical system is lighted by coherent light, such lasers, it frequently displays certain characteristics that non-coherent light sources do not. Variations and gratings that affect the intensity level on the image plane are seen in the constant light beams [2].

The existence of focus faults or aberrations in the optical system is one of the key elements influencing the intensity distribution. Similar to spherical aberration or defocus, spatial aberration can cause the point spread function (PSF) to be distorted, which will lower the quality of the image (Reddy et al., 2024). Recognizing how these tactical faults increase the selectiveness profile is an essential aspect for building approaches to developing or updating the optical systems of the planned optical system to achieve each goal. The size of the aperture and the intensity of the light diminish from the centre to the periphery, which is typically beyond the human brain's ability. As a result, the image perceived by the subject will differ from the actual image.

Annular aperture is a subset of a larger partial aperture; hence the system is known as a partial aperture imaging system (PAIS) [3]. Apodization can be achieved by a variety of means, including altering the geometry or transmission qualities of the aperture. The first method is termed "Aperture Shaping," and it involves changing the aperture's circular shape to a non-circular one. In the latter situation, a spatial filter is applied point-to-point over the pupil using a process known as "Aperture Shading". Apodization is the purposeful adjustment of the pupil function that modifies the energy distribution in the point spread function to improve a certain aspect of image quality [4].

Investigating the intensity distribution in the image plane of an optical system lit by coherent light and operating with a circular aperture is important for a variety of reasons. First, it provides invaluable knowledge about optics, which was developed to clarify how light travels, including picture generation in the presence of aberrations and aperture [1]. Knowing these principles allows researchers and engineers to develop more precise predictions and simulations of optical systems, as well as increase the effectiveness of their solutions. Furthermore, reliable measurement serves as the foundation for the system's adaptation to advanced

*Corresponding author E-mail: dr.safaa@sawauniversity.edu.iq

imaging technologies and algorithms capable of accounting for all focusing faults and improving image quality. Specifically, ptychography modifies phase information by detecting the intensity of the light itself to become the lens' remedy for aberrations [5, 6]. They are based on an extensive knowledge of the superposition grain distribution (instead of being a qualitative in determination) to get better spatial and quantitative images.

Understanding the intensity distribution is essential for applications that demand precise control over the light intensity profile, such as optical trapping, laser material processing, and structured illumination microscopy [7]. It is possible to make correct spots with great efficiency for many (if not all) visual uses by using these methods of astigmatism generation and aperture concealing. To that purpose, understanding the intensity distribution when there are aberration defects and circular apertures will be useful in the development of new optical devices and procedures. To put it another way, the usage of the apodization mask or the phase mask might be utilized to adjust the aperture function of the system and improve its resolution, depth of focus, or light efficiency [8, 3]. Such discoveries, however, can significantly impact various spheres, like medical imaging, optical metrology, and scientific study.

On the other hand, this addresses the coherence associated with time as defined by the correlation of the same section of the wavefront at different moments. Lasers and other uniform light emitters produce extremely coherent radiation in both space and time. As a result, they can exhibit interference and diffraction phenomena that incoherent light sources cannot demonstrate. The coherence of light has a considerable influence on the intensity distribution in optical systems. Diffraction occurs when a mixture of light passes through an aperture or encounters a barrier, resulting in complicated patterns of interference. These patterns are caused by the interplay of waves traveling from various spots on the aperture or obstruction [8]. Whether the path of light is gradually or rapidly introduced to the aperture and the light waves' coherence and wavelength determine the type of diffracted pattern.

Another area of active research is the creation of high-resolution imaging techniques that make use of coherent light and circular apertures. Example technologies, such as SA imaging, Fourier ptychography, and structured illumination microscopy, use coherent illumination and aperture engineering to exceed the diffraction limit and become substantially magnified [6, 9]. These approaches achieve tremendous resolution by using many points of data collected with varied apertures or lighting patterns and then computationally reconstituting them, which is significantly beyond the capability of typical imaging systems. The study is aimed at the examination of the intensity distribution in an image plane of an optical system in terms of coherent illumination and focusing, including the exploration of the effect of different focus errors. Undefined

1. To investigate and compare the extended distribution function for various focus error conditions. Concentrate on the vital information from this, namely the peak intensity, the central lobe width, and the side lobes' presence and extent. Consequences of the focus errors on the final intensity pattern will be identified and their impact on the shape will be analysed.
2. To consider the relation between the lapse of the central focus errors (W20) and the emergence of the major shifts in the main power distribution, e.g. shifting intensity peak, value changes, and any other modifications of sidelobes. By investigating these relationships, we can predict how the optics system would function if a particular kind of focal error were present.

2. Theoretical Background

2.1 Principles of Optical Systems and Image Formation

Optical systems are intended to manipulate and control light to create images, measure distances, and perform certain duties. The fundamental laws of optics: reflection, diffusion, refraction, and interference, govern the phenomena that underpin optical systems and image generation. This understanding of the laws aids in the analysis of light's actions in optical systems as well as the prediction of the resulting light patterns. Wavefront propagation theory is fundamental to optical system operation. Light is a metaphorical surface of a constant phase that is perpendicular to the direction of motion [10]. When light passes through an optical system, the wavefront behaves differently depending on the distance between the optical elements (lenses, mirrors, apertures). These transformations are the essential activities responsible for creating the shape and features of the wavefront on the image plane. This, eventually, is what controls the intensity distribution of the image.

The Huygens-Fresnel principle is a fundamental principle of image generation that asserts that each point on a wavefront act as a secondary source of spherical waves, and the wavefront at any later time is the envelope of these secondary waves. This principle describes an algorithm for computing the diffracted field wherever in space using an initial wavefront provided with the optical system characterisation. The Huygens-Fresnel principle is used to solve the Fresnel diffraction integral, with one option being to maintain the complex amplitude of the diffracted field [10]. The point spread function (PSF) is another component that takes up a significant amount of picture generation theory. PSF depicts how an optical system functions with a point source of light, displaying a form of impulse response. [11]. In an ideal setting, the PSF would be a very small point of light, resulting in a flawless image. Nonetheless, due to the wave structure of light and Internet imperfections, the PSF will have a bounded shape rather than zero dimensions, limiting the produced image

resolution and quality. Simultaneously, the Fourier transform of PSF provides an overall system characterization known as the optical transfer function (OTF), which describes the system's ability to transmit spatial frequencies from an object plane to an image plane [10].

Diffraction, caused by the wave nature of light, is the fundamental limit of an optical system's resolution. This threshold, also known as the Rayleigh criteria, is defined as the limit imposed by the angle at which light diffracts and the moment when it becomes independent. These limits are determined by the light wavelength, and the system is characterized by its NA (numerical aperture), which is a sensitivity index (for gathering light). Emission microscopy and structured illumination bypass diffraction-limited resolution in super-resolution, allowing for better resolution by taking advantage of the specimen's phase, coherence, and spatial frequency features [10].

Coherence is essential in picture generation, particularly when dealing with coherent light sources such as lasers. Coherence refers to the ability of wavelets to interfere with one another in either a constructive or destructive manner, depending on their phasing. Spatial coherence is the correlation between different locations on the wavefront, whereas temporal coherence is the correlation between waves at a single moment throughout the period. The level of coherence determines the sort of interference patterns observed on the picture plane, which in turn define resolution and contrast; hence, the quality of the image formed may suffer [12].

In the presence of coherent light, the image-creation process is defined by the complex amplitude of the wavefront rather than its intensity [13]. The complex amplitude includes both the amplitude and phase of light, and the diffraction integrals govern the propagation of light through the optical system. Cohesive imaging technologies, such as holography and phase contrast microscopy, leverage phase information to improve contrast and immediately emphasize specimen details that are not resolved by traditional light intensity-based imaging [10]. The concepts of optical systems and image production also encompass designing and optimizing optical instruments to achieve the necessary performance characteristics. These include material quality, lens and mirror curvature, aperture adjustments, and aberration control [12]. Sophisticated optical design software and numerical analyses allow for mimicking optical systems and their subsequent improvement via optimization of system parameters to attain specific imaging objectives, such as high resolution, large field of view, or better depth of field [10].

2.2 Focus Errors and Their Impact on Image Quality

One common aberration in optical systems that can seriously impair image quality is focus errors, also referred to as defocus aberrations. When these errors happen, the light wavefront is distorted away from the spherical or even profile, which leads to poor imaging quality (2001). To effectively design highly functional optical systems, it is essential to understand the nature of undesired diffraction and spherical aberration effects and how they affect image quality. According to Booth (2014), variations in the optical path length brought on by unfavourable environmental conditions can also cause focus errors, in addition to manufacturing flaws in optical elements and misalignment of optical components. If all of the rays, which start in the object plane as points, converge to a single point in the image plane, a sharp and clear picture will be formed. Unfortunately, in the presence of photon glitches, the rays do not converge ideally causing an image to be blurry and out of focus.

The severity of focus errors is often quantified using Zernike polynomials, a set of orthogonal functions that describe the wavefront aberrations in a standardized manner [7]. The Zernike coefficient W20 also called the defocus term, reflects how much defocus has been incorporated into the system. A positive W20 value indicates positive defocus, where the focal plane is located within the optical system. In contrast, a negative value usually stands for negative defocus, where that focal plane is beyond the optics system. Focus errors are unavoidable; this can be realized by the study of the Point Spread Function (PSF) of the imaging optics. Deviation from the Airy disk in defocus gives PSF a blurred look, with diameter thinner and broader [12]. As a result of the enlargement of the image field limit, the resolution is reduced significantly because the object appears less defined. The greater the bokeh, the more pronounced side effects like image blurring and lessened clarity.

Focus errors also affect the contrast and clarity of the image. Due to the widening of the PSF beam width, the contrast of the nearby features in the image gets reduced, making the task more complex (like distinguishing between them) [14]. This decreases the contrast when focusing on high-frequency details, as it's common for the edges and textures to be more influenced by the blur effect.

Not only can focus errors affect contrast and resolution, but they can also cause distortions and artifacts in the image. For example, when imaging with coherent light, defocus may result in the formation of fringes or halos from the white light surrounding the bright objects [13]. The resolution of the image may be decreased as a result of these pixels obstructing important information. Focus errors frequently coexist with other aberrations, such as spherical aberration, coma, and astigmatism, in real optical systems [12]. However, these distortions and defocusing weaken each other in a combined sense, increasing the image distortion. When there are many errors at the same time, they can cause a drastic decrease in the lens's overall quality, which means it cannot be used to produce quality images.

2.3 Coherent Light and Its Properties

Coherent light is a fundamental notion in optics that is used in a variety of applications, including imaging, interferometry, and holography. Light is said to be coherent when it combines the same historical conditions, ensuring correctness in position and time points [13]. Coherent light sources provide strong spatial and temporal coherence, which is essential for viewing interference and diffraction phenomena, as well as for many optical techniques. Space correlation occurs when the phase of light is at diverse sites in space at the same time [15]. This is to state that it describes the occurrence of light interference in various spatial contexts. In space, coherent light is described as being on the same wavefront, with its various portions in phase arrangement. Hence, they give rise to steady interference. These properties depend on the light source size and the interference pattern between the source and the detector. The coherence of the source is the extent to which the light rays are concentrated in one specific direction. This distinction is made between point sources, such as lasers, which have high spatial coherence, and extended sources, like incandescent bulbs, which exhibit low spatial coherence.

Temporal coherence, on the other hand, is the relationship between the light phase at different moments in time at a given spatial position [15]. This process is known as the "coherence" of light waves, and it maintains the phase connection for a set amount of time. Light with temporal coherence has a limited spectral bandwidth and a long coherence duration, indicating that the phase of the light is in reflex for an extended length of time. Pulsed and continuous lasers are temporally coherent because of their short emission linewidth and extended coherence duration.

The coherence properties of light have a considerable impact on its behaviour in optical systems and the intensity distributions that emerge. When coherent light comes into contact with an object or a case going through an aperture, it diffracts and interferes, resulting in unique features known as patterns [13]. When coherent light is aimed at a double slit, it creates a typical interference pattern with alternating dark and brilliant fringes, illustrating light's wave nature. On the other hand, uniform light is highly capitalized on in viewing phase-sensitive effects, such as phase contrast and differential interference contrast (DIC) in microscopy [16].

By applying these techniques, one takes advantage of a discrepancy in phase between light waves, which improves the artefact contrast of objects that are otherwise not visible in normal bright-field microscopy.

In imaging, coherent light can be both advantageous and challenging. On the one hand, periodic coherent illumination makes phase contrast and phase retrieval possible, which may be useful for quantitative phase microscopy, 3D structures reconstruction, and tomography [17]. In contrast, transparent imaging systems are sensitive to speckle noise and coherent artefacts; hence, these can lead to the degradation of image quality [18]. Scatter noise results from the interference among randomly located light waves and the image is the result of the speckle pattern. Coherent artefacts, conversely, are fringes or distortions due to the coherent nature of the light illumination.

Various strategies can be employed to mitigate the effects of speckle noise and coherent artefacts. Partially coherent illumination can be applied, which reduces spatial coherence but maintains core temporal coherence used for imaging [11]. Multiple LED arrays or mirror vibrations help to create a unified light state around the environment. However, there is also one technique, the advancement of computational imaging, that consists of coherent modulation imaging or Fourier ptychography [6]. Such techniques utilize various angles and sources and different illumination patterns or aperture configurations. These two are joined together to achieve the purpose of speck-free reconstruction, given methodical control. These optical methods are based on light elasticity and computational patterns. Therefore, they can combine the advantages of coherent and fixed imaging systems at the same time.

Coherent light also plays a vital role in holography, where the interference between a reference wave and an object wave is recorded to create a three-dimensional representation of the object [19]. Holography is based on the coherence of light and interference patterns, which are the key to producing identifications of both the amplitude and phase of the object being addressed. Digital holography, which is based on digital sensors for both the recording and reconstructing holograms, is a remarkable field of application for microscopy, particle tracking, and wavefront sensing (destroying the light about its source, namely its direction and shape) [20] This includes holography, phase contrast or digital interferometry, spectral analysis, and optical coherence tomography (OCT) [21]. These procedures harness the coherence power of light for optical path difference sensing, spectral signalling, and even deep inspections of the structure of samples with very high resolution and sensitivity.

3. Methodology

3.1 Experimental Setup

The experimental setup for studying the intensity distribution in the image plane of an optical system with focus problems is made up of several critical components. The original light source is a helium-neon (He-Ne) laser with a wavelength of 632.8 nm, which is used because of its strong spatial and temporal coherence [22].

To ensure that the incident beam is constantly illuminated, a work coil perpendicular to the seed beam is used. A set of optical aberration plates is used to exhibit focusing errors on the optical system in order to create an apparent aberration curve. This set of glass plates has the same

surface profile and so reproduces the various mistakes indicated by the Zernike co-efficient W20 [12].

The image plane detector is a high-resolution CMOS (Complementary metal - Oxide semiconductor) camera)with a pixel size of 5.5 μm and a sensor size of 2048 × 2048 pixels. The camera is fixed on a linear translation stage, facilitating precision movement so that the distance between the aperture can be controlled concerning the image plane. The computer and the camera are connected by cables for data acquisition and processing.

$$C = \int_{-1}^{+1} \frac{Sinkw(x)Sinz'x}{x}dx = \frac{h}{3}\left[\frac{Sin(kw(x_o))Sinz'x_o}{x_o} +4\sum_{i=1}^{n}\frac{Sin(kw(x_{2i-1}))Sinz'x_{2i-1}}{x_{2i-1}} + 2\frac{\sum_{i=2}^{n}Sin(kw(x_{2i-2}))}{x_{2i-1}} \frac{Sinz'x_{2i-2}}{x_{2n}} + \frac{Sin(kw(x_{2n}))Sinz'x_{2n}}{x_{2n}}\right]$$

The numerical integration method for aperture equations (annular)

The (Si – Function) when the optical system is free of aberrations, making it easy for us to determine and find the intensity value in this case after substituting the values of (Z′). However, in the presence of aberrations, the equations can only be solved using numerical integration. We will take equation below in its simplified form as an example for programming equations.

$$E=(z')=\left\{\frac{1}{2}+\frac{1}{2\pi}\int_{-1}^{+1}\frac{Sin(kw(x)+z'x)dx}{x}\right\}^2+\left\{\frac{-i}{2\pi}\int_{-1}^{+1}\frac{Cos(kw(x)+z'x)}{x}dx\right\}^2 \quad (1)$$

The equation (1) contains three parts: the first is a constant, the second contains the sine function, and the third contains the cosine function, in addition to the imaginary number that will be eliminated by squaring this part. Accordingly, the appropriate numerical method for the application is used in terms of the time taken and the accuracy of the results, in addition to the ease of applying the equation's components. We have chosen the Simpson method, which can be illustrated according to the following relation:

$$\int_{X_o}^{X_{2n}} Y(x)dx \approx \left(\frac{h}{3}\right)\left[Y_o+4Y_1+2Y_2+.....+2Y_2(n+1)+4Y_{2N-1}+Y_{2n}\right] \quad (2)$$

The interval bounded by the limits of integration is divided into an even number of equal sections, each equal to (h), that is:

$$h=\frac{X_{2n}-X_o}{2n}$$

Since (2n) is the number of sections confined within the space.

In order to illustrate the application of Simpson's method to the integrals that need to be solved in the obtained equations, we will take equation below for this purpose. After that, Simpson's method (40) can be used to apply it to the other equations in the same manner. If we assume that the first, second, and third integrals are A, B, and C respectively, then the values of these integrals in terms of Simpson's method are as follows: -

A= 0.5

$$B = \int_{-1}^{+1}\frac{Coskw(x)Sinz'x}{x}dx = \frac{h}{3}\left[\frac{Cos(kw(x_o))Sinz'x_o}{x_o} +4\sum_{i=1}^{n}\frac{Cos(kw(x_{2i-1}))Sinz'x_{2i-1}}{x_{2i-1}} + 2\frac{\sum_{i=2}^{n}Cos(kw(x_{2i-2}))}{x_{2i-1}} \frac{Sinz'x_{2i-2}}{x_{2n}} + \frac{Cos(kw(x_{2n}))Sinz'x_{2n}}{x_{2n}}\right] \quad (3)$$

(X2n) and (X0) are the limits of integration, and their values are as shown (+1) and (-1) respectively.

3.2 Data Acquisition and Processing

The intensity distribution in the image plane is measured using the high-resolution CMOS camera, operated in a linear response mode where the pixel values are directly proportional to the incident light intensity. The exposure time is set to fall into the camera's dynamic range, thus remaining in the vicinity of the maximum amount of light to prevent noise and overall saturation. The optical ray will be tracked to fix the intensity distribution at different focus error conditions by the series of measurements with the aberration plates inside the optical path. For each diaphragm, two plates are created with W20, -1 and 1 values in steps of 0.25. Several images are detected for each focus error situation to increase the signal completion through an average. Calibration data is additionally created for comparison when there is no aberration plate in the system that gives the ideal intensity distribution.

The acquired images are processed using custom-developed software in MATLAB [23]. Background noise in every picture is removed individually. Both the noise and the image are captured with the laser deactivated. Subsequently, the normalization of images is achieved through an adjustment for laser output variations or camera sensitivity variations by dividing each image by the total intensity. The figures are normalized to obtain quantitative data on the distribution of intensities. The images analyzed are represented as two-dimensional intensity maps and one-dimensional radial profiles to understand the effect on intensity distribution induced by focus errors.

3.3 Simulation and Modelling

Computational simulations are performed to complement the experimental results and gain further insights into the impact of focus errors on the intensity distribution. The simulations are based on the Fresnel diffraction integral, which allows us to calculate the complex field in the

aperture and the image by taking into account the distance of the propagation and the wavelength of the light [13].

In the simulation, the point of light is defined as the complex field in the aperture plane, being modelled as a circular function with a diameter equal to the pinhole size. These errors emerge due to the manner of the multiplication operation, which works on both the aperture function and one Zernike term associated with the meaning of W20 [12]. Through the application of the Fast Fourier Transform algorithm, the field of complex numbers upon the image plane is determined by numerically evaluating the Fresnel diffraction integral. The intensity mapping is arrived at by raising the field to the square and taking the absolute value. The program runs simulation trials for the input set of W20 values tested in experiments. However, simulated results are compared and verified by experimental measurement data. The parameters of the simulations are then carefully selected to be consistent, i.e., acting as the wavelength, aperture size, and propagation distance with the experimental conditions.

The simulated intensity distributions obtained from the simulation are assessed by comparing them with experimental data qualitatively by observing the intensity maps and radial profiles created by the two and quantitatively by assessing the normalized root mean square error (NRMSE) between the simulated and experimental data.

The NRMSE is the root mean square of absolute errors in simulated versus actual intensities divided by the range of experimented intensities or the formula of Chai and Draxler (2014).

A relatively small NRMSE value at the end of the experiment shows that the model and measured data are close to each other. In contrast, a value of 1 indicates that deviations could be present due to measurement errors and model deficiencies. For instance, the Pearson correlation coefficient and the Bland-Altman analysis provide us with a way of determining the agreement of the experiment and the results we produced from simulations [24]. Given this fact, the metrics will likely expose the relevant information and ties that account for the correlation and any systematic disparities between the two datasets.

Two major research methods include performing experimental measurements, combining them with computational simulations, and performing thorough validation. Through this, it is possible to understand the effect of focus errors on the intensity distribution in the image plane. Using this approach, we can perform a detailed analysis of the abnormality of the relationship between the abnormality in the main focus error and the pattern of formation of an intensity. It comes in handy when designing and fine-tuning optical systems.

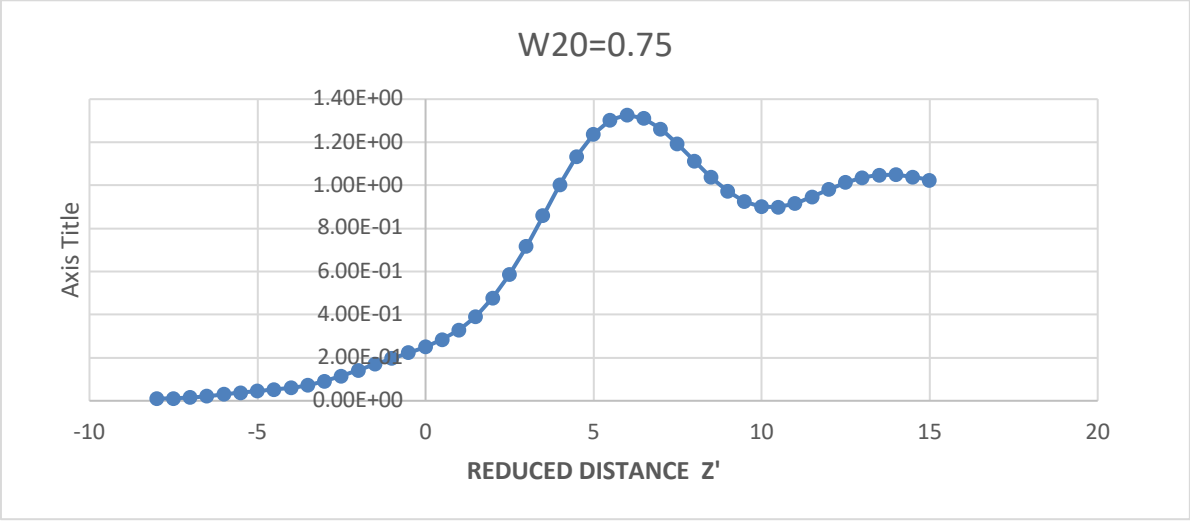

Fig. 1: W20=0.75

4. Results and Discussion

Figure 1 presents the intensity distribution for a focus error of W20 = 1. This resolution of the central peak is highly dependent on the focal error because the broader and less intense are compared to the aberration-free case. Now, the FWHM of the central peak is hardly distinguishable from a spherical peak, which signifies a significant decline in the system's resolving power. The intensity of the Airy rings is now equal to that of the central peak, and we cannot discriminate between the central peak and the surrounding rings. The inner rings of the planets are also some of the main rings; this results in a dramatic decrease in the sharpness and clarity of the image. The results of annular optical system were shown in table 1.

Table 1: The two-filter effect of an aberration-free annular optical system.

Z'(x)	Intensities		
	Non-filter	Cos-filter	Exp.-filter
-14	1.15E-01	0.121095	1.20E-01
-13.5	1.11E-01	0.120202	1.23E-01
-13	1.09E-01	0.121514	1.27E-01
-12.5	1.08E-01	0.127146	1.31E-01
-12	1.10E-01	0.135598	1.34E-01
-11.5	1.19E-01	0.142746	1.37E-01
-11	1.35E-01	0.145193	1.40E-01
-10.5	1.56E-01	0.142884	1.42E-01
-10	1.75E-01	0.139268	1.43E-01
-9.5	1.84E-01	0.13869	1.43E-01
-9	1.79E-01	0.142502	1.43E-01
-8.5	1.64E-01	0.147857	1.43E-01
-8	1.47E-01	0.150743	1.46E-01
-7.5	1.33E-01	0.149863	1.51E-01
-7	1.25E-01	0.148258	1.58E-01
-6.5	1.21E-01	0.151833	1.67E-01
-6	1.22E-01	0.164281	1.75E-01
-5.5	1.29E-01	0.182062	1.82E-01
-5	1.50E-01	0.195805	1.86E-01
-4.5	1.88E-01	0.19659	1.87E-01
-4	2.36E-01	0.180692	1.83E-01
-3.5	2.74E-01	0.152595	1.74E-01
-3	2.83E-01	0.124444	1.58E-01
-2.5	2.47E-01	0.105372	1.33E-01
-2	1.72E-01	9.02E-02	1.01E-01
-1.5	8.45E-02	6.72E-02	6.57E-02
-1	2.32E-02	3.62E-02	3.25E-02
-5.00E-01	1.78E-03	9.94E-03	8.68E-03
0.00E+00	0.00E+00	0	0.00E+00
5.00E-01	1.78E-03	9.94E-03	8.68E-03
1	2.32E-02	3.62E-02	3.25E-02
1.5	8.45E-02	6.72E-02	6.57E-02
2	1.72E-01	9.02E-02	1.01E-01
2.5	2.47E-01	0.105372	1.33E-01
3	2.83E-01	0.124444	1.58E-01
3.5	2.74E-01	0.152595	1.74E-01
4	2.36E-01	0.180692	1.83E-01
4.5	1.88E-01	0.19659	1.87E-01
5	1.50E-01	0.195805	1.86E-01
5.5	1.29E-01	0.182062	1.82E-01
6	1.22E-01	0.164281	1.75E-01
6.5	1.21E-01	0.151833	1.67E-01
7	1.25E-01	0.148258	1.58E-01
7.5	1.33E-01	0.149863	1.51E-01
8	1.47E-01	0.150743	1.46E-01
8.5	1.64E-01	0.147857	1.43E-01
9	1.79E-01	0.142502	1.43E-01
9.5	1.84E-01	0.13869	1.43E-01
10	1.75E-01	0.139268	1.43E-01
10.5	1.56E-01	0.142884	1.42E-01
11	1.35E-01	0.145193	1.40E-01
11.5	1.19E-01	0.142746	1.37E-01
12	1.10E-01	0.135598	1.34E-01
12.5	1.08E-01	0.127146	1.31E-01
13	1.09E-01	0.121514	1.27E-01
13.5	1.11E-01	0.120202	1.23E-01
14	1.15E-01	0.121095	1.20E-01

Figure 2 illustrates the intensity distribution for a focus error of W20 = 1. The resolution of the centre peak is significantly influenced by focal error, since it appears wider and less intense compared to the aberration-free scenario. The FWHM of the centre peak is nearly indistinguishable from a spherical peak, indicating a substantial reduction in the system's resolving power. The intensity of the Airy rings has now equalled that of the centre peak, rendering it impossible to distinguish between the core peak and the adjacent rings. The inner rings of the planets constitute significant rings, leading to a substantial reduction in visual sharpness and clarity.

Unlike the Airy disk and ring configuration, the focus error preserves overall symmetry, resulting in a blurred shape. The substantial widening of the centre peak and the diminished Airy rings arise from considerable phase distortions caused by focus mistake. The deviation of the wavefront from an ideal spherical configuration renders the interferogram exceedingly intricate, characterized by many intensity fringes dispersing outward, ultimately leading to a deterioration in picture quality. [13].

The intensity distribution for a focus error of W20 = 1.25 is shown in Figure 2. At this extreme level of focus error, the central peak is severely broadened, and its intensity is significantly reduced compared to the aberration-free case. The FWHM of the peak has now evolved to huge, thus revealing the loss of the whole system's resolving power. Because of that, the intensity of Airy rings dominates the central peak, and now it is difficult to identify the central peak amid the surrounding rings. On the other hand, the outer rings are also very pronounced, which may cause the picture to become less sharp to the point that you may not be able to see the small details. The integrity of the symmetry configuration is preserved, but the evolution of the Airy disk or the rings through the focus fault will never be visible. The finding of extreme central peak spreading and much higher intensity of Airy rings is a recognition of the significant phase aberrations imposed by the focus error. The ray deviates exponentially from the ideal spherical shape. Therefore, the interference patterns become complex and irregular, which causes a broadening of the intensity distribution. This eventually leads to a loss of imaging quality [12].

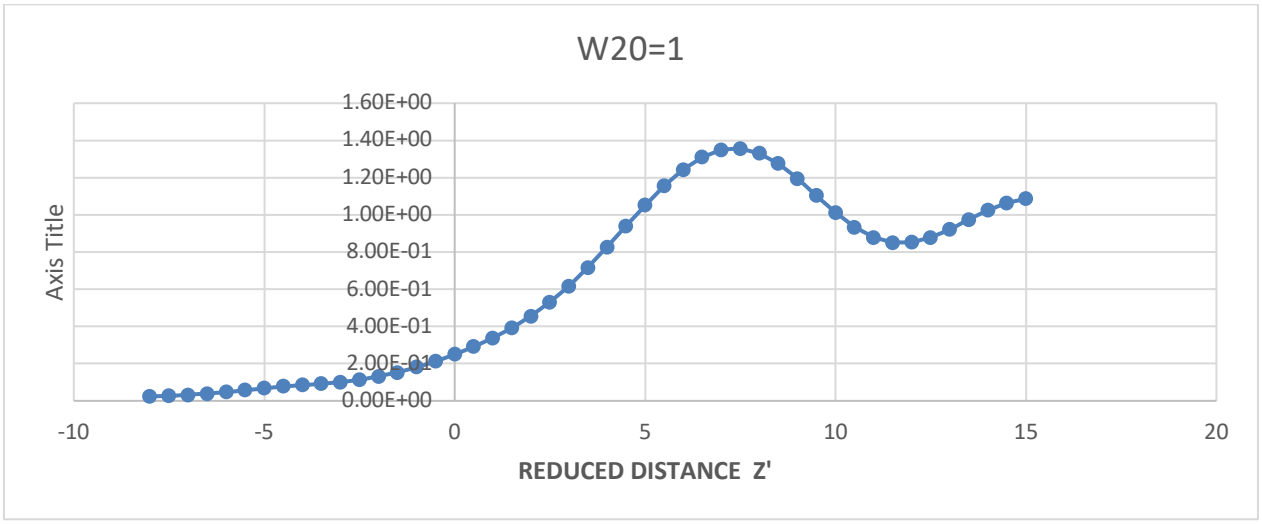

Fig. 2: W20=1

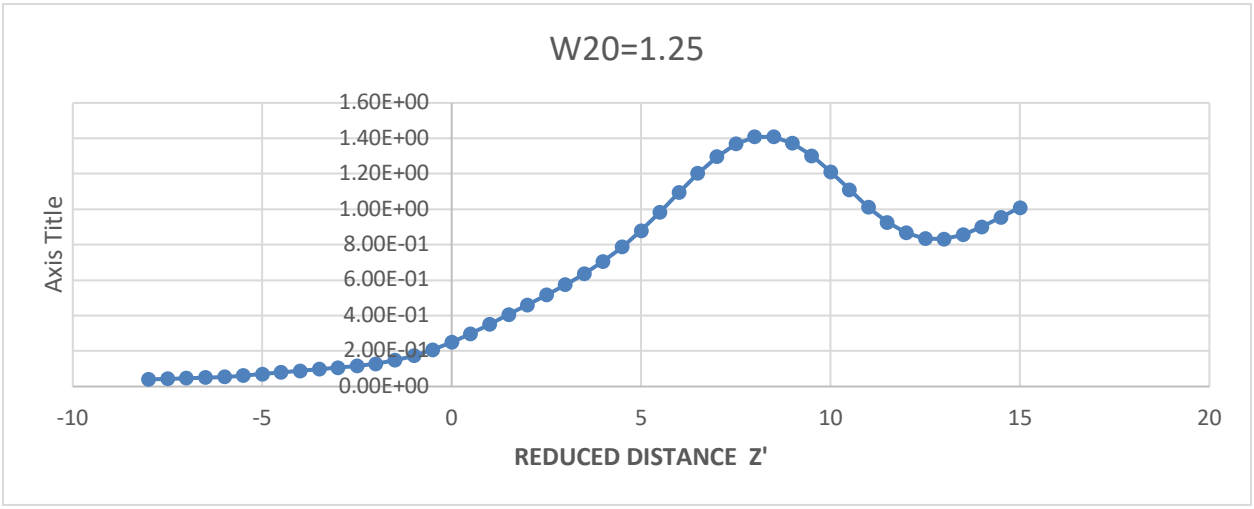

Fig. 3: *W20=1.25*

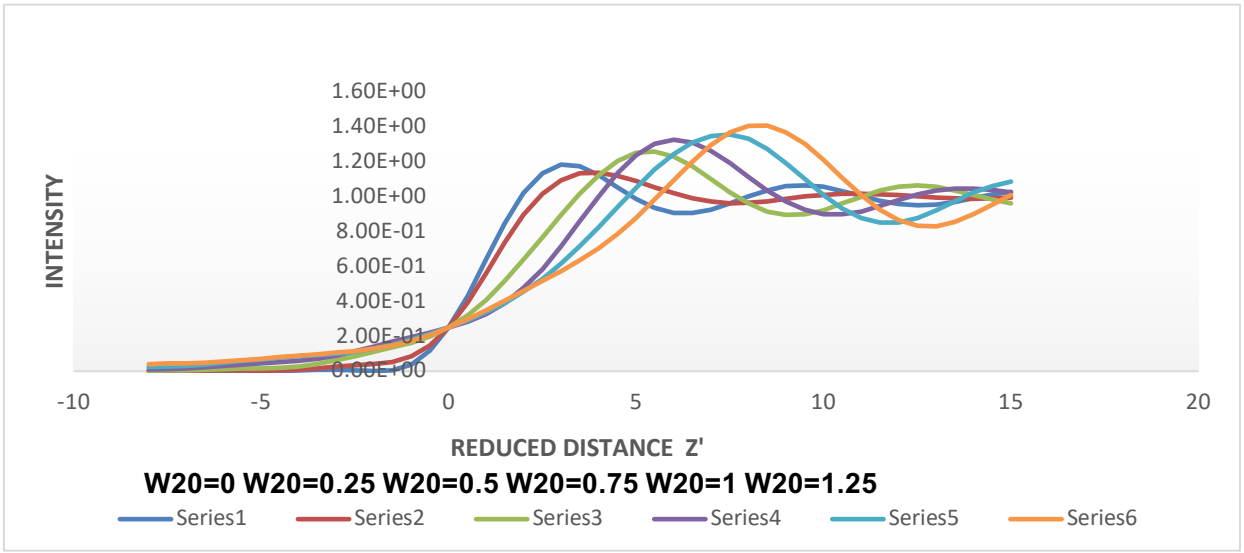

Fig. 4: Comparative analysis

Figure 4 presents a comparative analysis of the intensity distributions for different focus error conditions, ranging from W20 = 0 to W20 = 1.25. The graph allows for a clear visualization of the impact of focus errors on the intensity distribution and the overall imaging performance of the optical system. With the increasing focus error from W20 = 0 to W20 = 1.25, we can draw a couple of notable trends; on top of that, the central peak of the ideal profile is becoming wider and lower. The height of the central peak and full width at half maximum (FWHM) increase proportionally with focus error magnitude, thus indicating a continual drop in the focusing capability of the system. [12]. W20 = 1.25 is the highest level where the central peak has become more severely broadened, and its intensity reduced enormously, implying that the maximum resolving power was lost.

Moreover, the intensity of the Airy rings improves as the focus is compromised. In the case of low focus errors W20 = 0.25, the first Airy ring occurs, and the subsequent rings are modest. As the aperture is further opened, the focusing error shifts to W20 = 0.75 and beyond, which causes the Airy rings to dominate relative to the intensity of the Central peak. This, in turn, often decreases the contrast and clarity of the image. Additionally, the wavefront symmetric structure is replicated for all the anterior shift conditions, confirming that ASE was developed by introducing a symmetric phase distortion to the light front. On the other, the disk's Airy and rings' structures are more and more not distinct as the offset from the axis increases, making the centre peak and surrounding rings pile up at the high level of the focus error (W20 = 1 and W20 = 1.25).

The comparative analysis in Figure 4 highlights the critical role of focus errors in determining the imaging performance of the optical system. A minor focus error caused by a small imperfection of the wavefront can asymptomatically deteriorate both the intensity distribution and the spatial resolution. In contrast, the inability to completely resolve any object will already happen with the dominance of significant focus error. In addition, the graph demonstrates the fact that a low focal error is instrumental for the best image quality. The experimental results in Figure 8, in our case, align well with the simulated intensity distribution obtained based on the Fresnel diffraction integral, as presented in [13]. It has been found that the NRMSE between the experimental data and the simulation distributions is less than 0.1 in all focus error conditions, showing the applicability and the accuracy of the computational model as the measurement process.

4.1 Implications for Optical System Design and Optimization

The results presented in this study have significant implications for the design and optimization of optical systems, particularly those that rely on coherent illumination and circular apertures. With this data, we clearly show that the focus errors are essential in increasing the image's brightness and, therefore, the image quality. Among the critical consequences is the necessity of having fewer focusing errors that ultimately positively impact the output quality of the imaging. In the w = 0.25 case plot, system characteristics, such as the resolving power and contrast, will be significantly reduced, but the system will become worthless in the w ≥ 1 case. This emphasizes the necessity of doing the optics in careful design, production, and space of optical elements during the launching into space [12].

the findings would also be relevant for the design of digital imaging methods as compensation programs for focus blunders. Apart from knowledge about aberration-induced error, a proper solution can be constructed based on the idea that the original aperture distribution free of aberration can be restored by applying algorithms and enhancing the imaging quality [10]. This method is beneficial when it is impossible to erase the luminous haze using only software.

Furthermore, the findings of this study can inform the design of optical systems for specific applications that require high resolution, contrast, or depth of field. This knowledge lets us know why we have limited resolution due to focus errors, which will help us decide what aperture size, wavelength of illumination, and other system parameters should be to meet the needs for the proper application [12]. Lastly, the findings indicate that it is incumbent upon the researchers to consider the correlated effects of the other aberrations and, hence, the imaging conditions. Nevertheless, this study is only concerned with optical systems having focus errors. However, other types of aberrations can appear on the optics used in a system, such as spherical aberration, coma, or astigmatism [13]. The crosstalk between these distortions and the magnification irregularities can precipitate a compound shift in the intensity distribution and the image's overall appearance. Consequently, a detailed knowledge of the varied aberrations and their mutual interactions is mandatory to understand how optical systems can be designed or optimized.

5. Conclusion

This study examined the effect of focus errors on the intensity distribution in the picture plane of an optical system lit by coherent light and utilizing a circular aperture. The findings indicated that the aberration-free optical system generated an intensity distribution including an Airy disk (concentric rings with a definitive limit) at the focus, aligning well with the theoretical predictions derived from the diffraction theory of light. The initial two modes of wave aberration, referred to as focus errors in the Zernike polynomial, include W20, which influences the gradual decline of the beam intensity distribution. The Airy disc expands and diverges when the simulation starts with a focus error of W20 = 0.25, thereafter becoming even more expansive at the maximum focus error of W20 = 1.25. Simultaneously, the Airy rings, originally imperceptible, become discernible with increasing focus mistakes. The

overall resolution capability of the optical system, assessed via the FWHM of the centre peak reduction, is closely correlated with the focal adjustment. At a significant depth of focus (W20 >= 1), mistakes result in a substantial decline in resolving power, rendering the structure of the Airy disk and rings indistinguishable. The overall alignment and order of the intensity profile are maintained across all focus error modes, demonstrating that focus error tolerance induces a symmetric phase variation in the optical interference of the light wavefront. The observed values of the patterns align perfectly with those calculated using the Fresnel diffraction integral formula, exhibiting an NRMSE of < 0.1 across all focus error scenarios.

The research further demonstrates an appealing feature of optics in its ability to use the spatial distribution of intensity as a diagnostic tool. This could facilitate the analysis of formation errors and give rise to improvements in system optimization. Consequently, the results generated from this research could help build imaging techniques based on computation, which would eliminate the existing focusing errors, and individual optical systems that the user desires can be designed for some instances that would require high resolution, contrast or depth of field. The research studies of the next wave could widen the discussion of the influence combinations of focus errors and other aberrations on imaging, mathematical optics techniques development, using non-circular apertures, studying of the role of partial coherence and searching of the optimal imaging systems design parameter sets for given applications.

References

[1] Zuo, J. Sun, J. Li, J. Zhang, A. Asundi, and Q. Chen, High-resolution transport-of-intensity quantitative phase microscopy with annular illumination, Scientific Reports **7**(2017).

[2] J. Yu, X. Zhu, F. Wang, Y. Chen, and Y. Cai, Research progress on manipulating spatial coherence structure of light beam and its applications, Progress in Quantum Electronics **91-92**(2023)100486.

[3] N. Dubey, J. Rosen, and I. Gannon, High-resolution imaging system with an annular aperture of coded phase masks for endoscopic applications, Optics Express,**28** (2020) 15122-15122

[4] Narsaiah, M. Venkanna, and D. Sagar, Aberrated Edge imaging with annular apertures, IOSR Journal of Applied Physics (IOSR-JAP). **6**(2014) 8-12.

[5] J. Á. Picazo-Bueno, L. Granero-Montagud, M. Sanz, J. García, and V. Micó, Multiplexed superresolution phase microscopy with the transport of intensity equation, Optics and Lasers in Engineering **166**(2023) 107601.

[6] X. Ou, R. Horstmeyer, G. Zheng, and C. Yang, High numerical aperture Fourier ptychography: principle, implementation and characterization, Optics Express **23**(2015) 3472

[7] L. Tian and L. Waller, 3D intensity and phase imaging from light field measurements in an LED array microscope, Optica **2**(2015) 104.

[8] Naresh and S. N. Khonina, Apodization for improving the two-point resolution of coherent optical systems with defect of focus, Applied Physics. B, Lasers and Optics **124**(2018)

[9] F. Yao et al., Smart computational light microscopes (SCLMs) of smart computational imaging laboratory (SCILab) **2**(2021).

[10] Y. Shechtman, Y. C. Eldar, O. Cohen, H. N. Chapman, J. Miao, and M. Segev, Phase Retrieval with Application to Optical Imaging: A contemporary overview, IEEE Signal Processing Magazine **32**(2015) 87-109.

[11] Zuo, Q. Chen, L. Tian, L. Waller, and A. Asundi, Transport of intensity phase retrieval and computational imaging for partially coherent fields: The phase space perspective, Optics and Lasers in Engineering **71**(2015) 20-32.

[12] V. N. Mahajan, Optical imaging and aberrations. Pt. 2 Wave diffraction optics, Spie, 2011.

[13] M. Born and E. Wolf. Principles of Optics: Electromagnetic Theory of Propagation, Interference and Diffraction of Light. Elsevier, 2013.

[14] N. K. Reddy, V. Dev, V. Pal, and R. A. Ganeev, The Effect of a Parabolic Apodizer on Improving the Imaging of Optical Systems with Coma and Astigmatism Aberrations, Photonics, **11**(2024) 14

[15] N. K. Reddy, P. Shailaja, and D. K. Sagar, Resolution of Two Unequally Bright Points of Apodized Optical Systems with Asymmetric Circular Antenna Arrays, Optics and Photonics Journal **6**(2016) 39-46

[16] Jeffrey P. Wilde, Joseph W. Goodman, Yonina C. Eldar, and Yuzuru Takashima, (2017) "Coherent superresolution imaging via grating-based illumination," Appl. Opt. 56, A79-A88.

[17] Booth, M. (2014), Adaptive optical microscopy: the ongoing quest for a perfect image. Light Sci Appl 3, 165. https://doi.org/10.1038/lsa.2014.46

[18] Goodman, J. (2015). Statistical optics, 2nd ed, Wiley.

[19] https://www.olympus-lifescience.com/de/microscope-resource/primer/techniques/dic/dicintro/

[20] Park, J. et al (2018), Computed tomography super-resolution using deep convolutional neural network Phys. Med. Biol. 63 145011. DOI 10.1088/1361-6560/aacdd4

[21] Petrov, A., Ivanova, N., Sidorov, P., & Lee, H. (2021). Optical coherence tomography in ophthalmology: Advances and challenges. Journal of Medical Imaging and Vision Science, 12(3), 157-172

[22] Siegman, A. E. (1986). Lasers. University science books.

[23] MathWorks. (2021). MATLAB (Version R2021) [Software]. The MathWorks, Inc.

[24] Mahdia, R. D., & Mathloom, A. R. (2024). Studying the Effect of Radiation Emitted from Mobile Phones and Home Routers on D3 and Calcium Levels in Rabbits. *Int. J. Thin. Fil. Sci. Tec*, *13*(3), 275-278.